

Pinning regimes of grain boundary vortices in $\text{YBa}_2\text{Cu}_3\text{O}_{7-x}$ coated conductors

A. Palau,¹ T. Puig,¹ J. Gutierrez,¹ X. Obradors,¹ and F. de la Cruz^{1,2}

¹Institut de Ciència de Materials de Barcelona, CSIC, Campus de la UAB, 08193 Bellaterra, Spain

²Instituto Balseiro and Centro Atómico de Bariloche, CNEA, San Carlos de Bariloche, Rio Negro 8400, Argentina

(Received 16 March 2006; published 21 April 2006)

A comprehensive analysis of the processes limiting the magnetic and temperature dependences of the critical currents of $\text{YBa}_2\text{Cu}_3\text{O}_{7-x}$ coated conductors is presented. We conclude that an unexpected heterogeneous vortex matter associated with two interacting vortex species characterizes the flux dynamics in the H - T space: The Abrikosov-Josephson vortices (AJVs) nucleated on the grain boundaries and the Abrikosov vortices (AVs) localized in the grains. A crossover field separating a plastic motion of strongly interacting AVs- and AJVs from an individual pinning regime of AJVs has been identified.

DOI: [10.1103/PhysRevB.73.132508](https://doi.org/10.1103/PhysRevB.73.132508)

PACS number(s): 74.25.Sv, 72.90.+y, 75.75.+a, 81.07.-b

Coated conductors have emerged as a groundbreaking solution to fabricate long and flexible superconducting $\text{YBa}_2\text{Cu}_3\text{O}_{7-x}$ (YBCO) tapes. This is being achieved using complex processing techniques allowing the texture of a buffered metallic substrate to be replicated in the superconducting layer. The coated conductor can be visualized as a network of low-angle grain boundaries (GBs) separating superconducting grains.¹ As a result, superconducting matter in coated superconductors cannot be taken as a homogeneous system. It should be treated as a heterogeneous distribution of two vortex species: one consisting of Abrikosov-Josephson vortices (AJVs) pinned on the percolating grain boundaries² and the other of Abrikosov vortices (AVs), localized in the grains. Whereas different AV motion regimes have been identified in YBCO single crystals and thin films,³⁻⁸ the physical mechanisms associated with the motion of AJVs on GBs have been only recently elucidated.^{9,10} However, their possible contribution to the vortex dynamics in coated superconductors is not yet understood. In this brief report, we show that the field dependence of the critical current of YBCO coated superconductors is determined by the heterogeneous characteristics of the system, including the interaction between the two vortex species. Several YBCO coated conductors with different textures and thickness grown by pulsed laser deposition (PLD) on ion beam assisted deposition (IBAD) and rolling assisted biaxial textured (RABITS) substrates have been analyzed. For comparison purposes a $0.25 \mu\text{m}$ YBCO thin film grown by PLD on a strontium titanate oxide single crystal with a ϕ -scan full width at half maximum of 0.5° is also presented, film-a. The inset of Fig. 1 shows a saturated magnetic hysteresis loop measured for film-a at 5 K. Due to the field dependence of the critical current density J_c , the hysteresis loop presents a peak at $\mu_0 H_a = 0$, as expected for a superconductor thin film.¹¹ Then, the $J_c(H)$ dependence can be determined from one of the two saturated branches of the loop by using Eq. (1):¹²

$$J_c(H) = \frac{4M(H)}{w[1 - (w/3l)]} \quad (w < l) \quad (1)$$

where $M(H)$ is the saturated value of the magnetization at the applied magnetic field H and w and l are the lateral

dimensions of the sample. Figure 1 shows the typical $J_c(H)$ dependence for a thin film at different temperatures. Notice that J_c exhibits a plateau at low magnetic fields at all temperatures. Above a certain crossover field $\mu_0 H_{\text{cross}}^{\text{SC}}$, a gradual transition to a power-law behavior, i.e., $J_c(H) \propto H^{-\alpha}$, is detected. The field $\mu_0 H_{\text{cross}}^{\text{SC}}$ has been defined at the point where the power-law fit crosses the low-field plateau. This crossover field has been previously observed in thin films, single crystals, and irradiated single crystals,^{4,5,7,8} and it is associated with different temperature-dependent interactions between the vortex lattice and pinning defects.

The simplest critical current regime is detected for $\mu_0 H_a < \mu_0 H_{\text{cross}}^{\text{SC}}$, where the field independence corresponds to a single-vortex pinning regime,¹³ since the pinning energy is much larger than the vortex-vortex interaction. Thus, by equating the Lorentz and the pinning forces, $J_c B \sim n f_p$, where f_p is the individual pinning force per unit length, and n is the density of the pinned vortices, $J_c \sim f_p / \Phi_0$ is indepen-

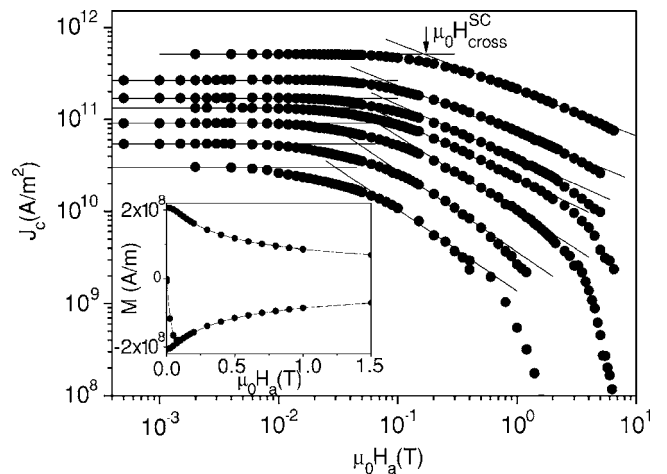


FIG. 1. Magnetic field dependence J_c determined for film-a at different temperatures. Data are fitted with the power-law behavior $J_c(H) \propto H^{-\alpha}$ at high fields with $\alpha = 0.5, 0.52, 0.58, 0.62, 0.82, 0.88$, and 0.88 at 5, 25, 40, 50, 60, 70, and 77 K, respectively. The arrow shows the crossover field $\mu_0 H_{\text{cross}}^{\text{SC}}$, determined at 5 K. Shown in the inset is a saturated magnetic hysteresis loop measured for the same film at 5 K.

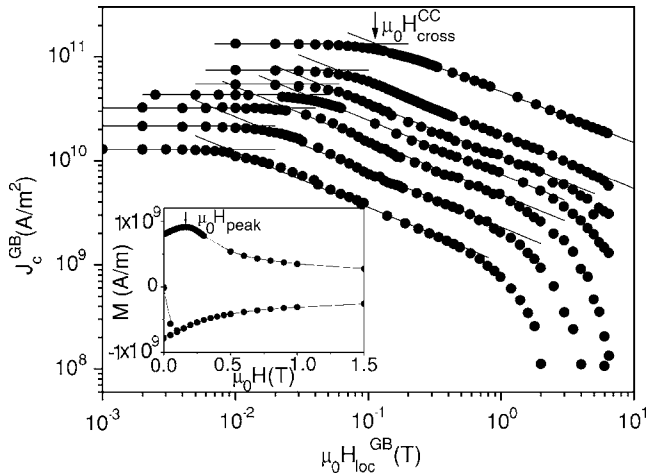


FIG. 2. J_c^{GB} as a function of the local field determined for the sample IBAD-a at different temperatures. Data are fitted with the power-law behavior $J_c^{\text{GB}}(H) \propto H^{-\alpha}$ at high fields with $\alpha=0.49, 0.51, 0.51, 0.52, 0.52, 0.53,$ and 0.53 at 5, 25, 40, 50, 60, 70, and 77 K, respectively. The arrow shows the crossover field $\mu_0 H_{\text{cross}}^{\text{CC}}$, determined at 5 K. Shown in the inset is a saturated magnetic hysteresis loop measured for IBAD-a at 5 K.

dent of B , in agreement with the experimental results. The field $\mu_0 H_{\text{cross}}^{\text{SC}}$, marks a crossover from an individual vortex pinning regime, to a collective pinning regime where vortex-vortex interaction cannot be disregarded. The power-law coefficient α obtained for the thin film analyzed increases with temperature, from $\alpha \sim 0.5$ at 5 K to $\alpha \sim 1$ at 77 K. Different values of α going from 0.5 to 1 have been reported for YBCO thin films grown on single crystals,^{4-6,8} though $\alpha \sim 1$ is expected for a pure collective pinning regime of linear defects while $\alpha \sim 0.5$ for the plastic pinning regime.¹³ At high fields, when the magnetic field approaches the irreversibility field, J_c decreases faster with increasing magnetic field and departs from the power law⁶ (see Fig. 1).

The inset of Fig. 2 shows a saturated magnetic hysteresis loop measured for a 1- μm -thick YBCO film PLD grown on a $\text{CeO}_2/\text{IBAD-YSZ}$ (Yttria-stabilized zirconia)/Ni-Cr stainless steel substrate with $\Delta\phi=5.7^\circ$,¹⁴ IBAD-a. Notice that in this case the magnetization peak occurs at a positive magnetic field value of the reverse branch of the magnetization loop instead of at zero applied field. This phenomenon has been previously ascribed to granularity effects in which case the local magnetic field at the grain boundaries is given by $\mu_0 H_{\text{loc}}^{\text{GB}} = \mu_0(H_a - H_{\text{return}})$,¹⁵ where H_{return} is the field trapped inside the grains returning through the grain boundaries. This leads to a hysteretic behavior of the grain boundary critical current density $J_c^{\text{GB}}(H_a)$, when we apply Eq. (1) to the ascending and descending branches of the hysteresis curves.¹⁶ This irreversibility will disappear when J_c^{GB} is plotted as a function of the local magnetic field, $J_c^{\text{GB}}(H_{\text{loc}}^{\text{GB}})$. We assumed $\mu_0 H_{\text{return}} = \mu_0 H_{\text{peak}}$, independent of the applied magnetic field, since at large fields, where the field dependence starts to be important, the contribution of the return field is negligible.¹⁷ We have also made sure, before determining J_c^{GB} , that the total magnetic moment measured in the hysteresis loops corresponded only to the magnetic moment asso-

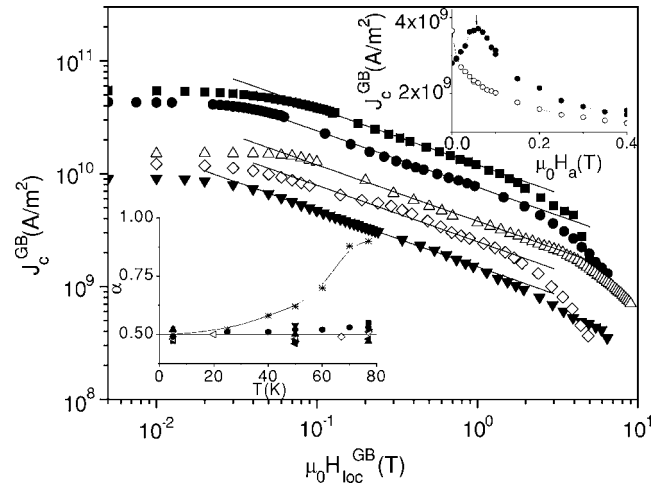


FIG. 3. J_c^{GB} as a function of the local magnetic field determined at 50 K for the coated conductors IBAD-a (●), IBAD-b (▼), IBAD-c (■), RABITS-a (◇), and RABITS-b (△). All data has been recorded inductively except for RABITS-b which corresponds to a transport measurement. Solid lines correspond to power-law fits $J_c^{\text{GB}}(H) \propto H^{-\alpha}$, with $\alpha=0.5$. Lower inset shows the temperature dependence of the exponents α determined for the film-a (*) and for a great variety of RABITS CCs (open symbols) and IBAD CCs (closed symbols). Upper inset shows the magnetic field dependence of the transport hysteretic J_c^{GB} determined for IBAD-d at 25 K on increasing (○) and decreasing (●) the magnetic field.

ciated with J_c^{GB} . The magnetic moment associated with the grain current loops can be neglected due to the small grain size compared with the sample size.¹⁵ We have determined the average magnetic grain radius a and the grain critical current density J_c^{G} for IBAD-a by using the methodology reported in Ref. 15. A temperature-independent value of $a \sim 1 \mu\text{m}$ has been found, which is clearly much lower than the sample dimension $5 \times 5 \text{ mm}^2$. The ratio $J_c^{\text{G}}/J_c^{\text{GB}}$ obtained at 77 K is $J_c^{\text{G}}/J_c^{\text{GB}} \sim 2.5$. These values give then a ratio $m^{\text{G}}/m^{\text{GB}} \sim 10^{-3}$.

Figure 2 shows the $J_c^{\text{GB}}(H)$ dependence obtained for IBAD-a at different temperatures. At a first glance the similarity between the data from Figs. 1 and 2 is obvious. A plateau in Fig. 2 similar to that observed for nongranular thin films is detected at low fields. At higher fields there is a crossover field above which a field dependence of the form $J_c^{\text{GB}}(H) \propto H^{-\alpha}$ is also observed. However, an important difference should be noted denoting different physics phenomena. In the coated conductor, the power-law field dependence is described by a temperature-independent, single value $\alpha \sim 0.5 \pm 0.05$.

Figure 3 shows the $J_c^{\text{GB}}(H)$ dependence at 50 K for IBAD-a, another IBAD film grown on the same substrate with thickness $t=1.6 \mu\text{m}$ and $\Delta\phi=12.7^\circ$, IBAD-b, and two RABITS coated conductors, RABITS-a and RABITS-b, grown by PLD on a $\text{YSZ}/\text{CeO}_2/\text{Ni-Mn}$ substrate¹⁸ with $t=0.8$ and $0.25 \mu\text{m}$, respectively, and $\Delta\phi \sim 6^\circ$. Additionally we have also included a $0.23 \mu\text{m}$ YBCO thin film deposited on a CeO_2 buffered IBAD-YSZ layer grown on a polycrystalline YSZ substrate with a $\Delta\phi=7.8^\circ$, IBAD-c. J_c^{GB} shown for RABITS-b has been obtained by transport measurements.

The upper inset of Fig. 3 shows the field dependence of the transport J_c^{GB} measured for IBAD-d with $t=1.2\ \mu\text{m}$ and $\Delta\phi=6.5^\circ$ at 25 K on increasing and decreasing the applied field, which reproduces the hysteresis obtained from inductive measurements. The results of Fig. 3 evidence that despite the different texture, thickness, and architecture of the coated conductors (different J_c^{GB}) the $J_c^{\text{GB}}(H)$ dependence is described by the same power law with $\alpha=0.5\pm 0.05$. The lower inset of Fig. 3 compares the α values, obtained from transport and magnetic measurements at different temperatures, for a variety of IBAD and RABITS coated conductors with those for the nongranular thin film-a. Contrary to the clear temperature dependence of α for film-a for all coated superconductors $\alpha\sim 0.5$. In coated conductors, the dislocation cores at the grain boundaries act as a linear array of columnar pinning centers. Since for a 5° boundary the distance between dislocations is $D\sim 4.6\ \text{nm}$ and thus the associated matching field would be $B_\Phi\sim 100\ \text{T}$,¹⁹ we can certainly assure that for the range of grain boundaries present in these coated conductors (5° – 12°) and magnetic fields applied, the one-dimensional (1D) AJV array of vortices is expected to be in the single-vortex pinning regime. Therefore, $J_c B\sim n f_p$, and since the motion of AJVs is dominated by a line of equally spaced defects of density $n=1/(ba_0)$, where $a_0=(\Phi_0/B)^{1/2}$ is the vortex lattice spacing and b is the GB width, then

$$J_c^{\text{GB}} = \frac{f_p}{b\sqrt{\Phi_0}} \frac{1}{\sqrt{B}} \quad (2)$$

in clear agreement with the experimental results. This dependence has been previously observed in YBCO thin films grown on bicrystal substrates⁹ and predicted for a network of strong pinning planar defects.¹⁰ From the experimental data we conclude that the dislocation cores at the grain boundaries provide the pinning potential that limits the displacement of the vortices nucleated on the GB and this effects lies at the origin of the difference with respect to thin films grown on single-crystal substrates. On the other hand, one would expect the limit of single vortex pinning to remain valid down to $\mu_0 H_a=0$. Surprisingly, this is not the case. At $\mu_0 H_a < \mu_0 H_{\text{cross}}^{\text{CC}}$, a plateau with J_c^{GB} independent of H is reached. By analyzing the values $\mu_0 H_{\text{cross}}^{\text{CC}}$ obtained for several IBAD and RABITS coated conductors and comparing them with the crossing field $\mu_0 H_{\text{cross}}^{\text{SC}}$, measured for film-a, we realize that $\mu_0 H_{\text{cross}}^{\text{CC}}$ is surprisingly similar to $\mu_0 H_{\text{cross}}^{\text{SC}}$, and that these values do not appreciably depend on the thickness of the YBCO layer or on the coated conductor architecture. This result indicates a clear correlation between $\mu_0 H_{\text{cross}}^{\text{CC}}$ (associated with AJV motion) and $\mu_0 H_{\text{cross}}^{\text{SC}}$ (associated with the crossover field of the grains, i.e., with the field above which the AV-AV interaction surpasses the individual vortex pinning interaction). In other words, the single-AJV behavior in the GB is sensitive to the elastic properties of the AV. Therefore, in this heterogeneous vortex system the one-dimensional individual pinning regime of AJVs cannot coexist with the single-vortex pinning regime of AVs.

The observed plateau at $\mu_0 H_a < \mu_0 H_{\text{cross}}^{\text{CC}}$ is understood by assuming that weakly pinned AJVs nucleated in the perco-

lating grain boundaries interact with strongly pinned AV neighbors located in the grains, in a configuration similar to the artificially patterned channels localized in between ion-irradiated superconducting banks described in Ref. 20. In this case the AJV motion requires overcoming the barrier induced by the AJV-AV interaction. Therefore, J_c^{GB} is reached when the Lorentz force equals the elastic force determined by the shear modulus c_{66} . Hence, $J_c^{\text{GB}}=2Ac_{66}/WB$,²⁰ where W is the width of the channel, A is a constant that takes into account anharmonicities in the lattice potential, and c_{66} is the shear modulus of the lattice given by $c_{66}=\phi_0 B/16\pi\mu_0\lambda_{ab}^2$,²⁰ resulting in a J_c^{GB} independent of B :

$$J_c^{\text{GB}} \propto \frac{2A\Phi_0}{16W\pi\mu_0\lambda_{ab}^2}. \quad (3)$$

In our case we consider the channel width W to be the grain boundary width b , i.e., the region affected by the stress field associated with the GB dislocation cores through which the AJVs move. Although a pure dislocation core in the YBCO can be considered one to two times the Burgers vector (~ 0.4 – $0.8\ \text{nm}$), the associated stress field has been determined to extend up to ~ 5 – $6\ \text{nm}$.^{19,21} Hence, by using $b=5\ \text{nm}$, $\lambda_{ab}(50\ \text{K})=220\ \text{nm}$, and A between $1/(2\pi)$ and $1/30$,²² we obtain values of J_c^{GB} between 5×10^{10} and $1\times 10^{10}\ \text{A/m}^2$, which are in agreement with the J_c^{GB} plateau values of Fig. 3. In this picture, the AVs hold the AJVs, retarding their motion until the Lorentz force surpasses the shear force. Remarkably, the experimental results indicate that a strongly interacting AV-AJV plastic system is encountered at low magnetic fields [plateau of $J_c^{\text{GB}}(H)$] while a system governed by individual pinning motion of AJVs in a 1D distribution of linear defects is attained at higher magnetic fields with $J_c^{\text{GB}}(H)\propto H^{-0.5}$. It is important to recall that the crossover field between these two regimes is triggered by the appearance of the collective vortex pinning regime at the grains. Within the collective pinning theory the decrease of the critical current is associated with an increase of the number of vortices that respond elastically to the presence of a force. Thus, because this volume increases with field the impedance to move vortices within the GB decreases and the individual pinning might take over as shown in experiments. The results provide clear evidence of the heterogeneous nature of superconductivity in coated superconductors.

Figure 4 compares the $J_c(H)$ dependence of film-a and $J_c^{\text{GB}}(H)$ for IBAD-a at 60 K. Since the value of J_c for the nongranular thin film decreases faster with increasing magnetic field than the value of J_c^{GB} for the coated conductor we can define another crossing field $\mu_0 H_{\text{joint}}$, which marks the point where the two critical currents merge. In this situation the current density necessary to move vortices located at the grain boundaries also moves vortices located inside the grains, i.e., $J_c^{\text{GB}}\sim J_c^{\text{G}}$. The same crossover field has been determined from transport measurements performed in bicrystals²³ and in coated conductors.²⁴

A general magnetic phase diagram for vortex motion in coated conductors (inset of Fig. 4) has been defined by determining the lines $\mu_0 H_{\text{cross}}^{\text{CC}}(T)$ and $\mu_0 H_{\text{joint}}(T)$. At low fields,

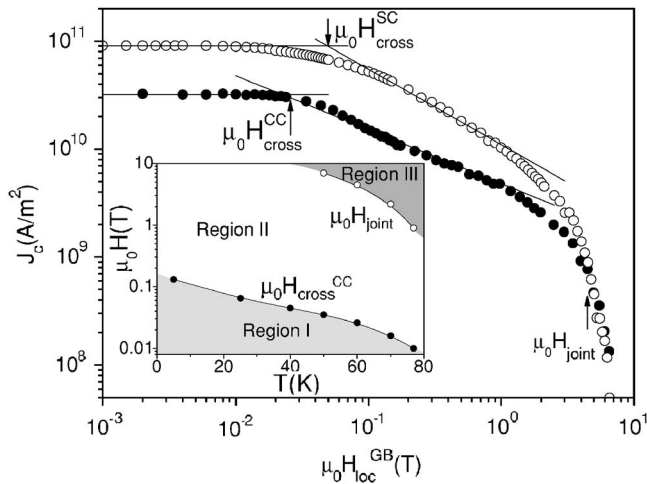


FIG. 4. Magnetic field dependence of J_c , obtained for film-a (○) and J_c^{GB} for IBAD-a (●) at 60 K. Arrows indicate the values of $\mu_0 H_{cross}^{SC}$, $\mu_0 H_{cross}^{CC}$, and $\mu_0 H_{joint}$ at this temperature. Shown in the inset is the general magnetic phase diagram of vortex motion determined for the coated conductor IBAD-a, where three different regimes are distinguished (see text for explanation of each regime). The experimental curves $\mu_0 H_{joint}(T)$ and $\mu_0 H_{cross}^{CC}(T)$ are indicated by open and closed symbols, respectively.

below $\mu_0 H_{cross}^{CC}$ (region I) only the motion of AJVs at the grain boundaries has to be considered ($J_c^{GB} < J_c^G$). In this case, the observed plateau of $J_c^{GB}(H)$ is understood assuming that AJVs move plastically in between strongly pinned AVs in the grains by overcoming the shear force. This indicates

that the AJV-AV interaction force is higher than the AJV pinning force. In the region between $\mu_0 H_{cross}^{CC}$ and $\mu_0 H_{joint}^{GB}$ (region II) motion of AJVs at the grain boundaries ($J_c^{GB} < J_c^G$) is attained although this is now associated with an individual pinning regime of 1D distributed linear defects, with $J_c^{GB}(H) \propto H^{-0.5}$. In this case the GB AJV pinning force is higher than the AJV-AV interaction force. At high magnetic fields, above $\mu_0 H_{joint}$ (region III), J_c^{GB} equals J_c^G and motion of both AVs and AJVs has to be considered. In this region vortex motion is not restricted within the GBs and thus the exponent $\alpha \sim 0.5$ can change to another value following the field dependence expected for the grains.

In summary, the magnetic field dependence of the critical current density in different YBCO coated conductors has allowed us to build up a general magnetic phase diagram where three different vortex motion regimes have been identified. We have determined a crossover field that separates a low-field region where AJV motion is dominated by their interaction with AVs in the grains (AJV plastic pinning regime) from a region governed by a single-AJV pinning regime, at higher fields. At high magnetic fields, motion of both AJVs and AVs has to be considered.

Support from CICYT (Grant No. MAT2002-02642), Generalitat de Catalunya Grant No. (2001-SGR-00336), CeRMAE, and EU (SOLSULET Grant No. G5RD-CT2001-00550 and HIPERCHEM Grant No. NMP4-CT2005-516858) is acknowledged. A.P. thanks MEC for partial financial support and F. d. I. C. wishes to thank MEC for a sabbatical stay. We would like to thank H. C. Freyhardt and B. Holzapfel for samples supply.

¹D. M. Feldmann *et al.*, Appl. Phys. Lett. **77**, 2906 (2000).

²A. Gurevich *et al.*, Phys. Rev. Lett. **88**, 097001 (2002).

³L. Civale *et al.*, Phys. Rev. Lett. **67**, 648 (1991).

⁴B. Dam *et al.*, Nature (London) **399**, 439 (1999).

⁵J. M. Huijbregtse *et al.*, Semicond. Sci. Technol. **15**, 395 (2002).

⁶F. C. Klaassen *et al.*, Phys. Rev. B **64**, 184523 (2001).

⁷L. Krusin-Elbaum *et al.*, Phys. Rev. B **53**, 11744 (1996).

⁸E. Mezzetti *et al.*, Phys. Rev. B **60**, 7623 (1999).

⁹A. Diaz *et al.*, Phys. Rev. Lett. **80**, 3855 (1998).

¹⁰A. Gurevich and L. D. Cooley, Phys. Rev. B **50**, 13563 (1994).

¹¹A. Sanchez and C. Navau, Phys. Rev. B **64**, 214506 (2001).

¹²D. X. Chen and R. B. Goldfarb, J. Appl. Phys. **66**, 2489 (1989).

¹³G. Blatter *et al.*, Rev. Mod. Phys. **66**, 1125 (1994).

¹⁴A. Usoskin *et al.*, IEEE Trans. Appl. Supercond. **11**, 3385 (2001).

¹⁵A. Palau *et al.*, Appl. Phys. Lett. **84**, 230 (2004).

¹⁶A. Palau *et al.*, IEEE Trans. Appl. Supercond. **13**, 2599 (2003).

¹⁷A. Palau, Ph.D. thesis (2005) <http://www.tdx.cesca.es/TDX-1201105-143027/>.

¹⁸B. De Boer *et al.*, Acta Mater. **49**, 1421 (2001).

¹⁹M. F. Chisholm and S. J. Pennycook, Nature (London) **351**, 47 (1991).

²⁰H. Pastoriza and P. H. Kes, Phys. Rev. Lett. **75**, 3525 (1995).

²¹A. Gurevich and E. A. Pashitskii, Phys. Rev. B **57**, 13878 (1998).

²²A. Pruyboom *et al.*, Phys. Rev. Lett. **60**, 1430 (1988).

²³S. I. Kim *et al.*, Phys. Rev. B **71**, 104501 (2005).

²⁴L. Fernandez *et al.*, Phys. Rev. B **67**, 052503 (2003).